3-DOF MR-Compatible Multi-Segment Cardiac Catheter Steering Mechanism

A. Ataollahi, R. Karim, A. Soleiman Fallah, K. Rhode , R. Razavi, L. D. Seneviratne, *Member, IEEE*, T. Schaeffter, K. Althoefer, *Member, IEEE*

***Abstract*—This paper presents a novel MR-compatible 3-DOF cardiac catheter steering mechanism. The catheter's steerable structure is tendon driven and consists of miniature deflectable, helical segments created by a precise rapid prototyping technique. The created catheter prototype has an outer diameter of 9 Fr (3 mm) and a steerable distal end that can be deflected in 3D space via four braided high-tensile Spectra® fiber tendons. Any longitudinal twist commonly observed in helical structures is compensated for by employing clockwise (CW) and counter clockwise (CCW) helical segments in an alternating fashion. A 280 µm flexible carbon fiber rod is used as a backbone in a central channel to improve the structure's steering and positioning repeatability. In addition to the backbone, a carbon fiber tube can be inserted into the structure to a varying amount capable of changing the structure's forcibility and, thus, providing a means to change the curvature and to modify the deflectable length of the catheter leading to an extension of reachable points in the catheter-tip workspace. A unique feature of this helical segment structure is that the stiffness can be further adjusted by appropriately tensioning tendons simultaneously. An experimental study has been conducted examining the catheter-tip trajectory in 3D space and its positioning repeatability using a 5-DOF magnetic coil tracking system. Furthermore, MRI experiments in a 1.5 Tesla scanner confirmed the MR-compatibility of the catheter prototype. The study shows that the proposed concept for catheter steering has great potential to be employed for robotically steered and MR-guided cardiac catheterization.**

I. Introduction

CARDIAC catheterization is a minimally invasive procedure performed by inserting a catheter tube through a small incision into the femoral vein and advancing the catheter through the vein into the heart. During this interventional procedure, the goal is to reach specific locations inside the heart and to perform examinations or treatments, such as electro-physical studies or radio frequency (RF) ablation of cardiac arrhythmia. The number of degrees of freedom (DOF) for a standard catheter is limited as it can only rotate and slide through the punctured point in the artery [1], [2]. Most commercial catheters consists of a flexible plastic body and a maneuverable tip that is manipulated using pre-configured guide-wires and a single tendon [3],[4] allowing a deflection of the catheter tip in one direction only. Using concentric combination of precurved elastic tubes has improved the manoeuvrability of the ore-configured catheters by increasing the number of degrees of freedom and controllability [5]. More advanced steering concepts have been proposed by industry [6]-[8] and a number of commercial products such as, the Artisan Extend™ Control Catheter allowing the adjustment of its tip position in three dimensions using 4 tendons have been developed recently [19]. Until recently, the integration of additional functionality came at the cost of a larger outer diameter (e.g. Hansen Medical's Artisan catheter system which has an outer diameter of 11.5 Fr) and the need for a metallic steering shaft to ensure sufficient catheter rigidity [9].

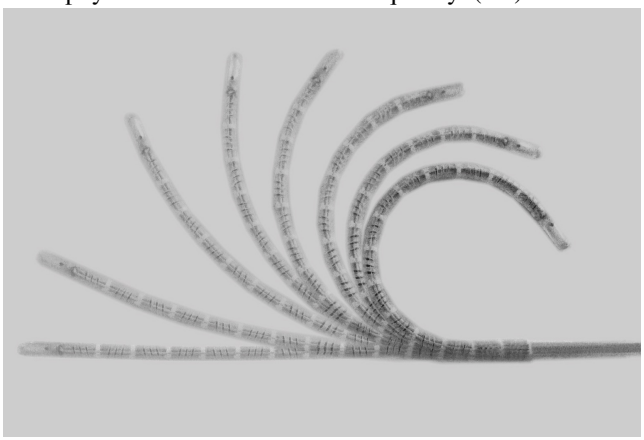

Fig. 1. The prototype steerable mechanism.

Cardiac catheterization is usually guided using X-ray fluoroscopy to visualize the device inside a patient's body. Despite the high temporal and spatial resolution of X-ray fluoroscopy, it can provide images with poor soft tissue contrasts of the anatomy. In addition, the patient and medical staff are exposed to hazardous x-ray radiation [10]-[12], which can become an issue in complex procedures requiring long exposure time. During the last decade many efforts have been undertaken to advance the field of Magnetic Resonance Imaging (MRI) towards image-guided interventions [13] and first clinical applications have been demonstrated [10]. In

This work was supported in part by Wellcome Trust and EPSRC under Grant WT088641/Z/09/Z.

A. Ataollahi, A. Soeliman Fallah, and K. Althoefer are with Centre for Robotics Research (CoRe), Department of Informatics, King's College London, Strand, London WC2R 2LS, U.K. (e-mail: ali.ataollahi@kcl.ac.uk; arash.soleiman-fallah@kcl.ac.uk; k.althoefer@kcl.ac.uk)

R. Karim, T. Schaeffter, R. Razavi, and K. Rhode, are with the Division of Imaging Scieneces, Department of Biomedical Engineering, King's College London, London, SE1 7EH, UK. (rashed.karim@kcl.ac.uk; tobias.schaeffter@kcl.ac.uk; reza.razavi@kcl.ac.uk; kawal.rhode@kcl.ac.uk)

L.D. Seneviratne is with Centre for Robotics Research (CoRe), Department of Informatics, King's College London, Strand, London WC2R 2LS, U.K. and the College of Engineering, Khalifa University of Science, Technology & Research (KUSTAR), Abu Dhabi, U.A.E. (e-mail: lakmal.seneviratne@kcl.ac.uk)

contrast to x-ray, MRI avoids ionizing radiation, offers excellent soft-tissue contrast and the ability to obtain anatomical as well as quantitative physiological information. Examples of procedures that will benefit from a MR-guided approach include treatments for congenital heart disease [14] and electrophysiology (EP) procedures [15]. However, the main roadblock for a widespread clinical use of MR-guided interventions is the limited number of MR-compatible devices [16]. Materials suitable for x-ray fluoroscopy are not necessarily compatible with MRI scanners. Many ferromagnetic materials cannot be used in the MR-environment due to the generation of significant artifacts that can deteriorate the MR signal considerably. Furthermore, conductive wires which are usually used for steering and to enforce mechanical stability, can result in excessive heating during RF transmission [17]. Recently, novel concepts have been integrated into a electrophysiology catheter and MR-safety has been demonstrated [18]; However, the steerability of the developed device was limited. To the best knowledge of the authors, the proposed catheter steering concept is the first of its kind, providing 3-DOF steerability in a catheter tip as small as 9 Fr, whilst, in addition, achieving MR compatibility.

II. Catheter Design

The following functional requirements are considered for the proposed catheter steering mechanism to be used for cardiac catheterization procedures.

1) MR-compatibility: Ferromagnetic material should be avoided to ensure MR-safety and diagnostic image quality. Furthermore long conductive wires cannot be employed in mechanical structure, since those would potentially lead to excessive RF-heating.
2) Diameter: Desired diameter of the catheter should be between 7 and 10 Fr (2.3 mm to 3.3 mm).
3) Flexibility: The steerable section of the catheter should be flexible enough to avoid possible injuries of vessel wall.
4) Stiffness: Adjustability of stiffness can help in EP-procedures to ensure providing adequate contact force of the catheter tip with endocardium.
5) Maneuverability: The mechanism should provide efficient and accurate steering of the catheter tip to a wide range of points inside the heart, without the need of twisting the catheter shaft.
6) Repeatability: Accurate relocation of the catheter-tip to reach a position in 3D space should be ensured.
7) Control technique: The catheter steering mechanism should be designed to be adoptable to both robotic and manual actuation systems.
8) Costs: A low-cost disposable steering mechanism is another important objective, as it will avoid sterilization issues and aid commercialization.

The work described here attempts to achieve the above requirements as much as possible. One of the main challenges was to meet many requirements without the use of metallic components, which are usually employed for mechanical stability and steerability. The proposed catheter steering mechanism consists of multiple stacked segments capable of deflecting along two axes. In addition, a sliding carbon fiber tube is employed to modify the curvature radius adding an additional degree of freedom. This is because of the less flexibility of the carbon fiber tube which blocks a number of segments from being deflected as a result of tendon actuation. The aim of the carbon fiber tube is to improve the catheter-tip navigation and enhance the tip force by providing support for the flexible manipulator. Stiffness adjustability is an additional feature of our design.

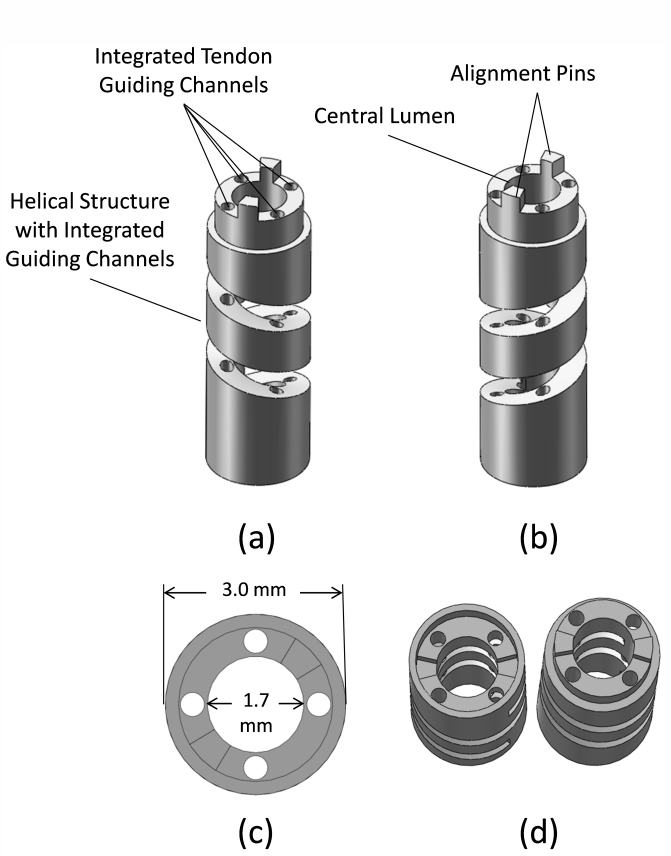

Fig. 2. (a) Schematic view of a clockwise (CW) segment. (b) Schematic view of a counter clockwise (CCW) segment. (c) Cross section view of a segment. (d) Bottom view (left) and top view (right) of a segment.

A. Segment Design

The presented catheter steering structure is made of multiple segments stacked together to shape a long steerable catheter tip (see Fig.1). Each segment, as shown in Fig. 2, has a helical structure with a length of 9 mm. The outer diameter of each segment is 9 Fr (3 mm) and the inside lumen has an inner diameter of 1.7 mm allowing the insertion of other optional elements. Each segment has three complete helical turns with a helical pitch of 1.55 mm and spring gap of 0.45 mm. The helical pitch value and the amount of gap within the spring structure are selected based on fracture analysis of the segments under different tendon load configurations. Several

designs have been investigated through trial-and-error and the optimized configuration has been opted in to meet the stress conditions. The spring-like behavior of each segment is leading to a deflection away from the plane spanned by applied normal force and the structure's longitudinal axis. Next to the inner lumen along the longitudinal axis, four tendon guiding channels with a diameter of 250 µm are incorporated within each segment, allowing the insertion of the steering tendons through all segments (Fig.2 (a)). The alignment indentations at the top of each segment are designed such that when they fit into the corresponding slots at the lower end of the subsequent segment, segments are perfectly aligned and form a continuous structure with continuous tendon guiding channels (See fig.2 (b)). The size of the steerable distal end of the catheter may vary based on the application. Thanks to its segment-based design the overall length of the steerable structure can be easily modified by employing a different number of stacked segments depending on the application.

The manufacturing process used to create the proposed miniaturized segments is challenging due to the requirements in mechanical stability and spatial size. There are only a limited number of methods available to produce such a small prototype. Most currently available manufacturing methods do not have the ability to produce parts with 250 µm channels with the required accuracy. MR-compatibility of material is another crucial requirement, which limits the choice of production methods. Therefore, the helical segments were created in this research project using a state-of-the-art rapid prototyping machine (Projet HD-3000 Plus, 3D Systems), which employs a large number of printing jets (680 jets) to create 3D objects with the resolution of 750 x 750 x 1600 DPI (xyz). The polymer material used to print the segments is a non-conductive ABS polymer (Acrylonitrile Butadiene Styrene) and thus MR-compatible.

This manufacturing method ensures the production of complex components with high precision. Ultra high precision, time efficiency, as well as low manufacturing costs are the most significant advantages of using rapid prototyping techniques for miniaturized robotic applications.

B. Steering Mechanism Assembly

For the prototype described here, fourteen segments (seven CW and seven CCW segments) have been made and stacked together to create a steerable catheter tip of 112 mm length (see Fig.1). The segments are attached in such a way that the tendon guiding channels are perfectly aligned. Fig. 3(a) shows the schematic of 3 segments assembled to form a steerable mechanism. The cutaway section view of the assembled steering mechanism is presented in Fig. 3(b). Inside the inner lumen there is a concentric assembly of two tubes and a thin rod. The outer tube is a 1.6 mm flexible tube made using a controlled heating process inside a laboratory oven (45 minutes @ 90°C) applied to a 2.5 mm Polyolefin heat shrinkable sleeve (Maplin, UK). The flexible tube is located inside the lumen providing the first layer of the inner lumen. Inside the flexible guide tube a carbon fiber tube (Woolmer Forest Composite, UK) with an outer diameter of 1 mm and an

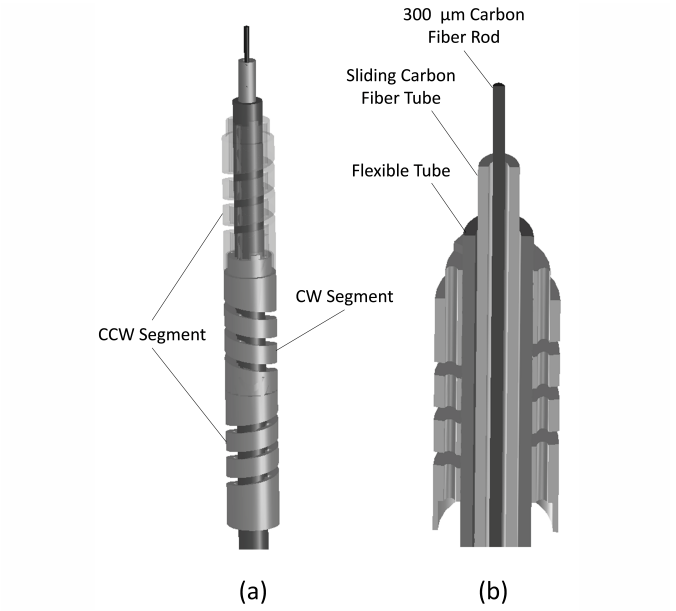

Fig. 3. Schematic of three segments stacked together in catheter distal assembly (a). Cut section of assembly (b).

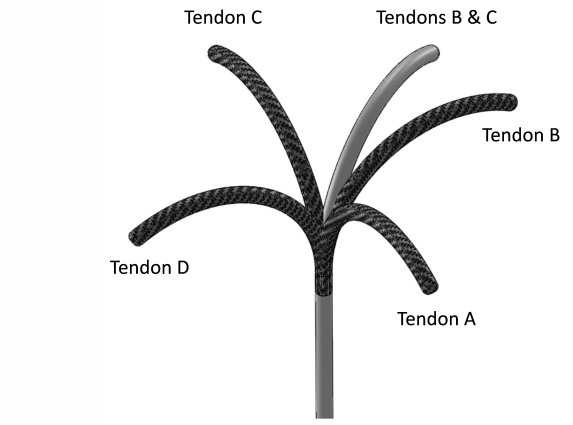

Fig. 4. Steering configurations related to actuation of the tendons A, B, C, and D. individual and combined configurations of tendons B and C are depicted as an example.

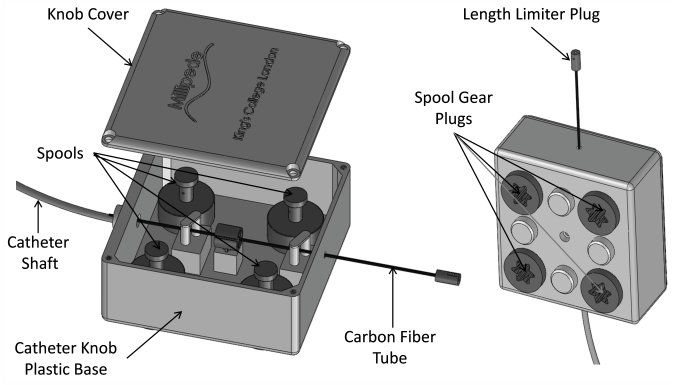

Fig. 5. The catheter control knob design (left). The spools' Gear Plugs (right).

inner diameter of 500 µm is inserted. The flexible guide tube is designed to allow the carbon fiber tube to move freely inside the lumen without damaging the segments potentially caused by the friction between the carbon fiber rod and the sharp edges of the helical segment turns.

The sliding carbon fiber tube is employed to control the deflectable length of the catheter. Because the carbon fiber tube is more rigid than the helical structure, moving the carbon fiber tube in and out of the catheter structure, its deflectable length is reduced and increased, respectively, and, thus, the bending curvature is reduced and increased, respectively. The carbon fiber tube is only 100 mm long, therefore, in order to actuate this linear axis from the catheter's control knob it is attached to a 1 mm glass fiber rod (Woolmer Forest Composite, UK) which is almost of the same length as the whole catheter and is attached to a control knob at the proximal end of the catheter allowing to slide the carbon fiber tube forward and backward, in and out of the steerable part of the catheter.

Additionally and along the most central, longitudinal line of the catheter structure, a carbon fiber rod with the diameter of 280 µm (Woolmer Forest Composite, UK) is inserted. This carbon fiber rod with a length of 120 mm is not controlled, but intended to improve repeatability of deflection by increasing the stiffness of the segment structure. One end of carbon fiber rod is fixed to the tip segment of the catheter (last segment of the steering mechanism) and the other side is located inside the carbon fiber tube in such a way that by sliding the carbon fiber tube it does not move in relation to the segments. Four braided high-tensile Spectra® fiber (Polyethylene fiber) lines are used as actuation tendons (0.15 mm Spectra® Fiber, Power Pro USA) and passed through the tendon guiding channels. This configuration allows the deflection of the steerable catheter structure along two axes (two degrees of freedom (2 DOF)). Fig. 4 shows the schematic relation between tendon actuation and the catheter deflection in 3D space.

When a force is applied to the top plane of a helical spring whilst its bottom plane is fixed, the top plane translates in line with the applied force, but also "twists" sideways because of the spring-like nature of the employed helical segments. This small rotation of each segment would add up in an assembled structure and could cause a considerable longitudinal twist along the overall catheter structure, if only CW or CCW helical segments were employed. Such complex non-planar twist in the structure would require complicated positioning control since it causes non-planar deflection. Therefore, this issue is addressed here by using an equal number of clockwise (CW) and counter clockwise (CCW) helical segments assembled in an alternating way. This configuration which effectively consists of paired CW and CCW segments compensates for the rotation of each segment along the assembly and results in an in-plane deflection. Fig. 3(a) shows the CW and CCW segments in the catheter assembly.

The complete catheter prototype that has been used in our experiments is developed employing a 2.4 mm monofilament reinforced tubing (Precision Extrusion, Inc., USA). This tube

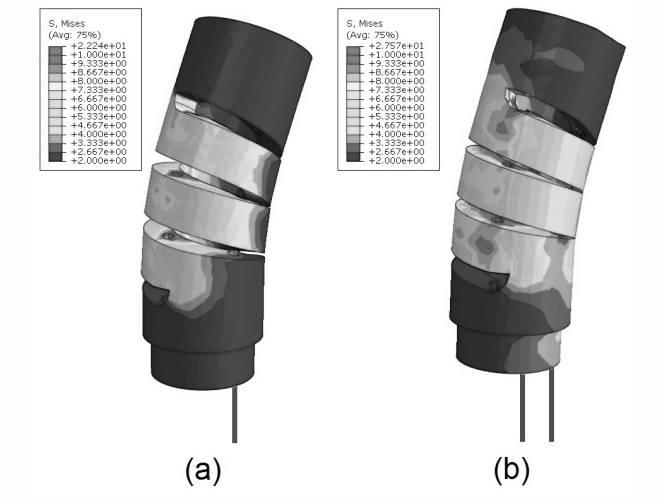

Fig. 6. Finite Element (FE) analysis results (von Mises stress contour) of a prototype spiral segment under a single tendon actuation (left) and simultaneous dual tendon actuation (right).

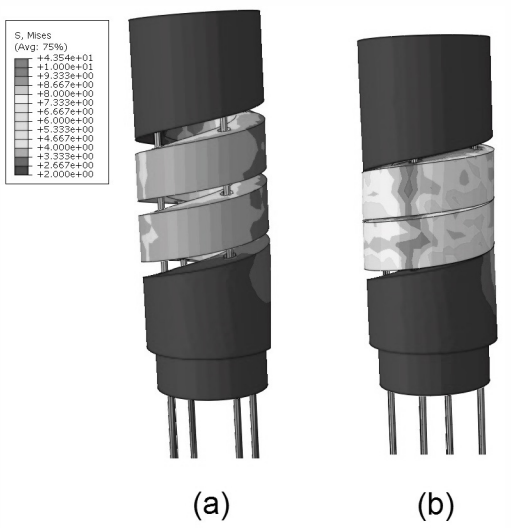

Fig. 7. (a) FE stress analysis of the segment under total force of 0.5 N applied simultaneously by four tendons. (b) Fracture analysis of a segment under simultaneous four-tendon loading using FE. Von Mises stress contours depicted.

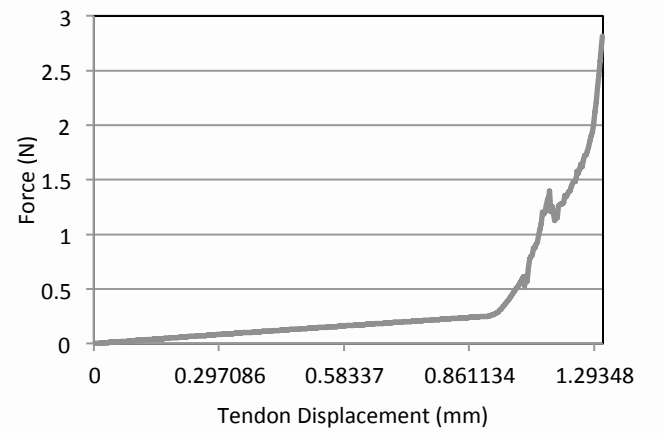

Fig. 8. Force-Displacement diagram during the segment fracture analysis until the point of complete closure.

which is connecting the steerable distal of the catheter to the control knob is called catheter shaft here. The length of the catheter shaft is 80 cm and can accommodate the tendons and glass fiber rod in its 1.8 mm inner lumen. A plastic catheter knob is developed and the catheter is integrated with the knob to form a plug and play catheter steering system. Fig.5 shows the catheter knob design. The knob consists of four spools to wind each tendon around a 6.4 mm (diameter) pulley. The catheter's 3rd DOF, carbon fiber tube, is also integrated to the knob in such a way that the whole catheter assembly can be easily plugged in to the robotic actuation device. Since all catheter components are made of plastic, non-conductive, and short length low-conductive (carbon fiber) materials the catheter can be used in MRI scanner safely.

III. Finite Element Analysis

A detailed finite element analysis of the helical segment was performed to investigate the deflection of an individual segment under force applied by a single tendon, two adjacent tendons, and four tendons simultaneously (ABAQUS Ver 6.9-1). The material used in the manufacturing of the segments was ABS-like plastic (VisiJet® X). Physical and mechanical properties of this material used in simulation were adopted from the manufacturer's manual as follows: Density=1040 kg/m^3 , Young's Modulus (E)=2168 MPa, Poisson Ratio= 0.25, Tensile Strength= 49 Mpa, Fracture Energy = 246 J/m [www.3dsystems.com]. For the sake of modeling hyperelastic behavior was assumed so that finite strain can be accommodated. The structural design (helical pitch, helical gap, spring geometry) is optimized in order to maximize strength at the helical section where the segment is deflected. A force in the range of 0 to 0.7 N is applied to a single tendon in the first analysis. Fig. 6 (a) shows the stress analysis results using a single tendon. The maximum stress in the whole structure is calculated to be 22 MPa, ensuring a reliable design, considering that the ABS material's tensile strength is 49 MPa. Fig. 6 (b) shows the stress analysis when the total amount of load equally applied to both tendons ranges from 0 to 1.2 N (0.6 N each tendon). In this case the maximum stress is calculated to be less than 28 MPa which is less than 57% of the material's tensile strength.

Further we tested our claim that the proposed steering mechanism is stiffness adjustable. Changing the stiffness can be achieved applying an equal force to all four tendons simultaneously. However, the amount of force or displacement of the tendons is limited by the segment's resilience. Fig.7 (a) shows the helical segment under a total tendon force of 0.5 N. The FE analysis shows the maximum stress to be less than 18 Mpa (again clearly below the material's tensile strength). The total tendon force then increased until the internal spring faces are in contact beyond which point excessive force is required to further compress the spring. Fig.7 (b) depicts the status of spring at the point of incipient complete closure. Fig. 8 shows the force-displacement curve up to this point and there was no fracture or loss of integrity observed in the four-tendon loaded segment. Fracture was simulated using brittle fracture model as a built-in capability in ABAQUS where fracture initiates following a convex hypersurface in the space of normalized

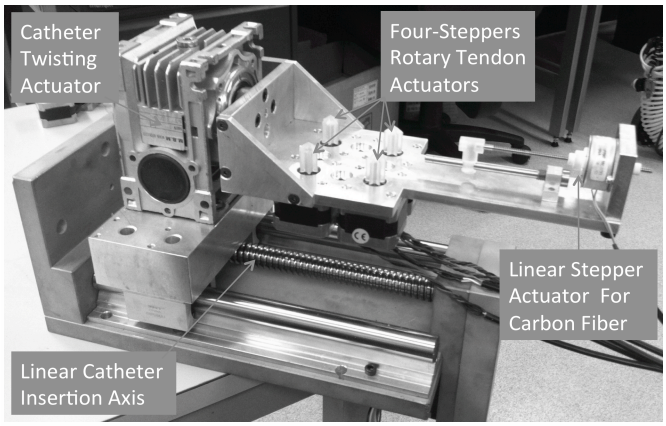

Fig. 9. 5-DOF Robotic Actuation Device.

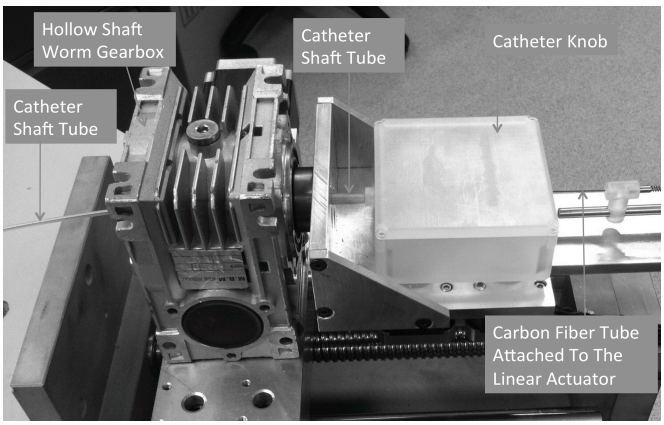

Fig. 10. 3-DOF catheter installed on the robot.

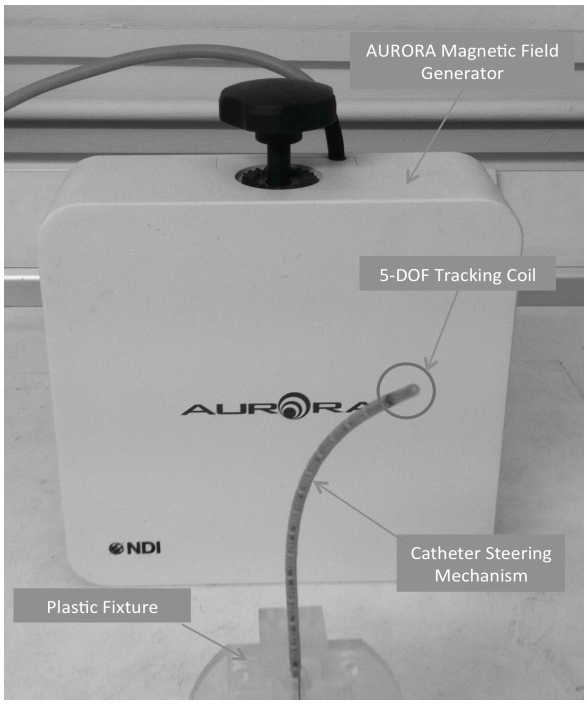

Fig. 11. Tracking coil integrated Catheter trajectory experimental setup.

nominal stress components and propagates by fracture mechanics dictated principles. The maximum von Mises stress at the point of closure is evaluated to be bounded to 43 MPa which is below the tensile strength of the ABS material. The FE analysis of the segment fracture proves the safe steering and stiffness adjustment of the catheter steering mechanism.

IV. Experimental Setup

A. Experimental Setup for Trajectory Measurements

In order to study the catheter tip workspace and positioning accuracy, the catheter prototype is connected to a robotic actuation device with four stepper motors (PK246PDA, Oriental Motor) shown in Fig. 9. The motors are attached to a gear which fits into the catheter's spool pulley for the 2-DOF tendon actuation. A linear stepper motor (FL 35BYZ-B01) is employed to actuate the 3rd axis by linearly moving the carbon fiber tube in and out of the central lumen. An additional, fourth axis is provided employing a hollow-shaft worm gearbox which can rotate the catheter (this axis was not used for 2-DOF catheter). The fifth degree of freedom describes the catheter translation. The structure is made of metal components and all axes are driven by stepper motors, therefore, it is not MR-compatible. This actuation system is only used for actuation analysis and kinematic validation and cannot be employed inside MRI scanner. The robotic device with integrated 3-DOF catheter is shown in Fig.10. As it is shown in this figure the catheter shaft passing through the hollow shaft of the worm gearbox (with a hole size of 8 mm in diameter) can be inserted into the sheath.

Stepper drivers (UIM24002 & UIM24004) are used to drive the stepper motors. The proposed stepper drivers are supporting a 16-micro-stepping mode which improves the rotational resolution 16 times to 3200 pulses/rev in the tendon actuators. Considering the spool pulley diameter which is 6.4 mm, theoretically, tendon displacement resolution of 6.2 µm per each step should be achieved; however, the measured tendon displacement using a caliper for stepper motion command of 100 pulses is measured to be 0.69mm (6.9 micron/step). The control pulses are generated using an industrial motion controller board (HICON, VITAL Systems Inc. USA) through Ethernet communication. A C#.Net code is developed for communication with the motion controller and operating the robot. The developed control software is modified to meet the requirements of each experiment. The joystick controlled remote operation feature is also integrated into the catheter navigation software. The control system at this stage is a simple open-loop control algorithm.

A commercial magnetic coil tracking system (NDI Aurora® EM) with a 5-DOF coil is used to measure the position of the catheter-tip in the experimental setup. For this the tracking coil with a diameter of 0.9 mm and a length of 9 mm is attached to the tip of the catheter during the trajectory experiments. The sensor can show the position of the catheter tip as well as its orientation in 3D space. The RMS position accuracy of the tracking system is claimed to be 0.70 mm for 5-DOF tracking sensor by the manufacturer [20]. However, from a separate experiment conducted in our test environment, the measurement accuracy was found to be 0.9 mm. The

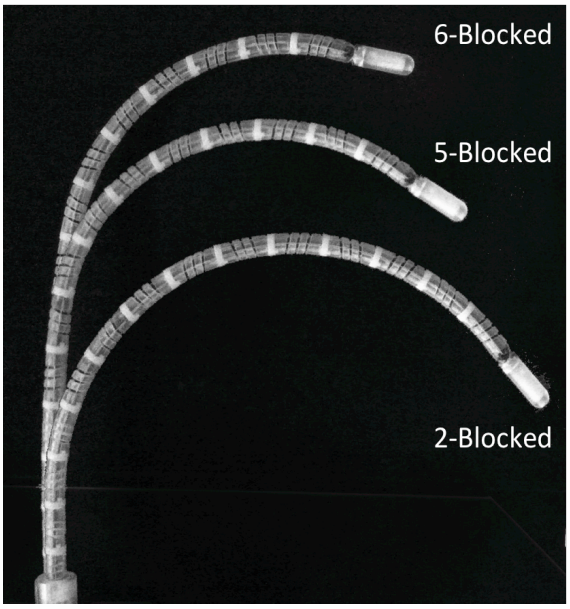

Fig. 12. Deflected prototype catheter in three different steerable length configurations. Two segments , five segments, and six segments are blocked.

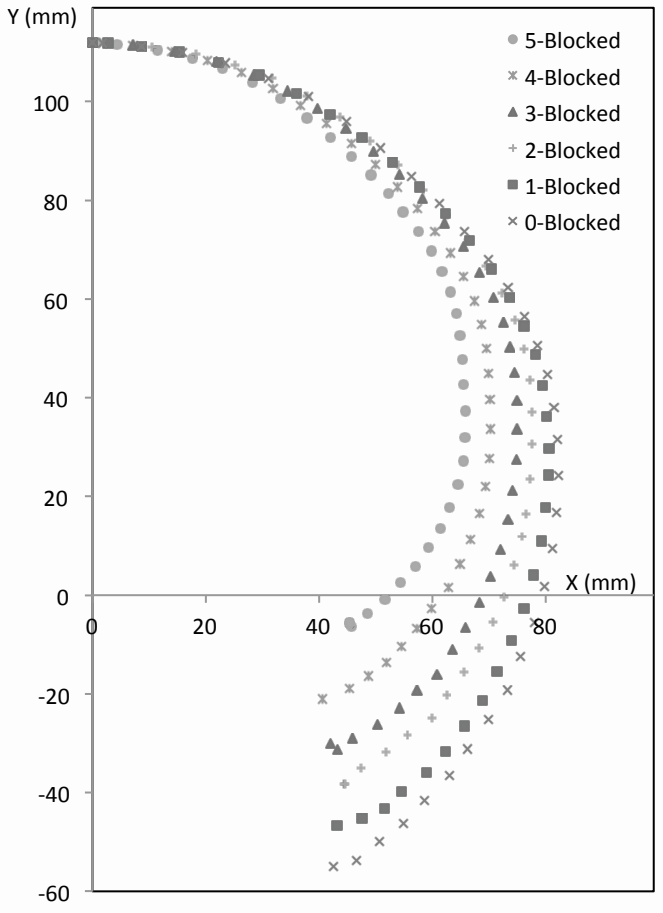

Fig. 13. 2D tip trajectory of the catheter in 6 different length-limiter configurations.

accuracy of the RMS orientation measurement is evaluated to be 0.28˚ (0.20˚ claimed by manufacturer [20]). The tracking information is recorded using our control software through RS-232 communication with the Aurora magnetic tracking system. An average of 10 readings is acquired for each recorded position. Since the magnetic tracking system is very sensitive to electromagnetic distortions, the robotic actuator is kept away from the tracking field and the catheter steering mechanism is fixed on a wooden table using a plastic fixture oriented in parallel to the magnetic field. Fig.11 shows the experimental tracking setup. The complete catheter with an 80 cm MR-compatible catheter shaft is employed; hence, the achieved results are obtained based on the behavior of the entire prototype in a realistic scenario. The recorded position information of the catheter-tip is used to study the 2D and 3D catheter-tip trajectories using one or two tendons. For a 2D trajectory measurement the catheter is positioned in a configuration in which its deflection occurs using the selected single tendon in the XY plane parallel to the magnetic field generator front surface. Repeatability and hysteresis effect of the steering mechanism are evaluated.

B. Stiffness Adjustability Experimental Setup

An experimental setup using a commercial force sensor (ATI Nano 17) and a linear stage (KK40-2001, Hiwin) is employed applying lateral forces to the catheter by moving the force sensor against the catheter-tip and recording the force-displacement values. The catheter's deflectable part is fixed to the table and the applied force based on the force sensor displacement is recorded. This setup was used to study the effect of variation in deflectable length on lateral forcibility. In addition it is used to investigate the stiffness adjustability feature of the presented prototype by increasing the tension in all the tendons simultaneously. This feature is believed to increase the stiffness of the catheter where increased forcibility is required.

C. Experimental MR-Compatibility Test Setup

The proposed catheter prototype is tested on the potential effects on MR image quality [11]. A major issue is local distortion of the main magnetic field homogeneity due to susceptibility of the material and potential metal contamination during the manufacturing process. For this a water-filled phantom with the catheter device (including the steering mechanism, catheter shaft, and control knob) is measured inside a 1.5 Tesla scanner (Philips Achieva). The main field homogeneity is estimated from a field map by acquiring two images at two different echo times (TE (echo delay time) =2.5/7.5 ms) and calculating phase difference of both images that contain real and imaginary components. The phase difference at each pixel is proportional to the resonant frequency at this location.

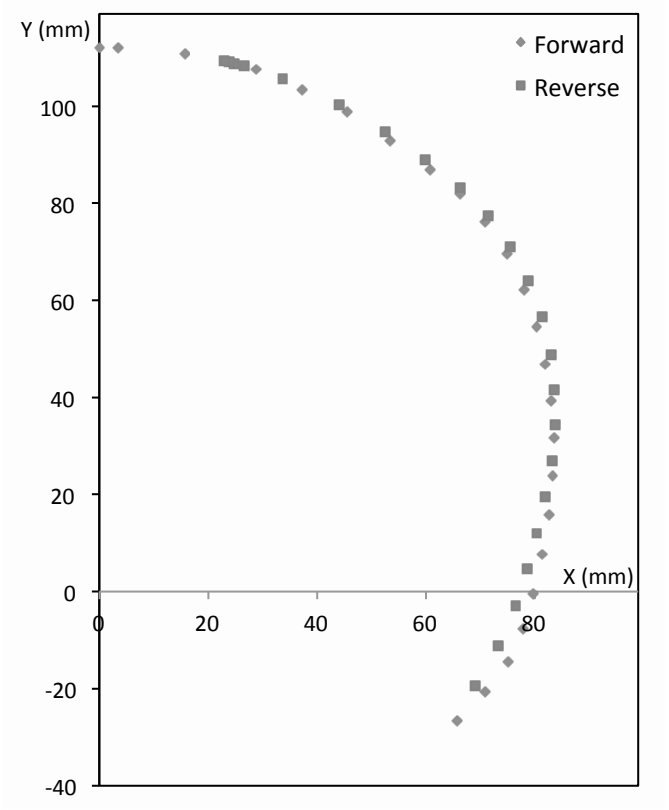

Fig. 14. Hysteresis experiment results by full deflectable length catheter.

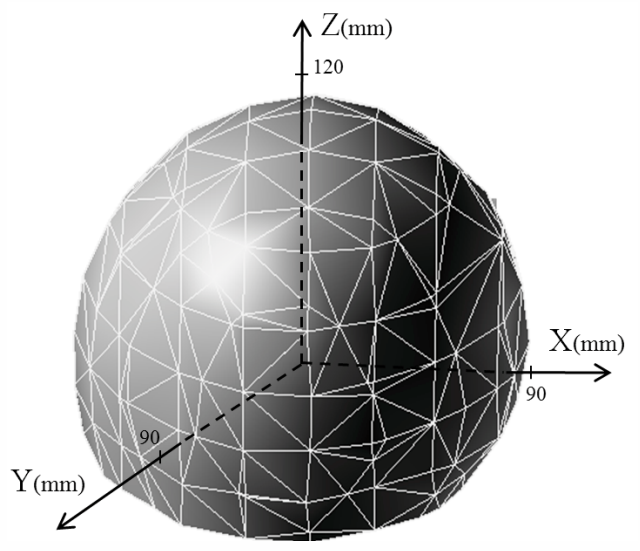

Fig. 15. A 3D tip trajectory experiment result demonstrates the workspace of the catheter-tip in full deflectable length where the length limiter axis is not employed.

V. Experimental Results

A. Planar Catheter-Tip Trajectory

Figure 12 shows the prototype catheter in three different deflectable length configurations. The in-plane trajectory of the catheter-tip using a single tendon is presented in Fig. 13. For this experiment the tendon has been actuated from the

initial state up to 16 mm in steps of 0.4 mm displacements. The position data presented here is the average of 10 position readings which is received from the magnetic tracking device for each point after catheter was stable in each position. The effect of using a length-limiter axis (3rd DOF) in 6 different deflectable-length configurations is also shown in this figure. Starting with the full deflectable length of the steering part, the set of tip positions is shown as "0-Blocked" in Fig. 13. The presented curve shows the trajectory of the catheter-tip without any limitation in deflectable length. Then by advancing the carbon fiber tube into the catheter lumen and limiting the deflectable length by means of blocking the first helical segment the next set of points is recorded which is referred as "1-Blocked" in this figure. Repeating the experiment by blocking more and more segments all six sets of points are recorded and presented (Fig. 13). As a result of using the integrated length-limiter, the catheter can extend its reach in the 3D space without the necessity of axial movements. Besides, this additional axis provides extra support for the catheter when more force is required to be applied when the tip is in contact with tissue.

B. Deflection Hysteresis Analysis

The trajectory of the catheter-tip during a forward and reverse tendon displacement is recorded using the same experimental setup to measure potential hysteresis effects using a full length deflection configuration. Similar to the trajectory experiment, the tendon is displaced up to 16 mm in steps of 0.4 mm and then released along the same steps in reverse until it reaches again the initial state; during this operation, the resultant tip positions are recorded. Fig.14 shows the catheter tip trajectory during the forward and reverse deflections. The experiment shows that the hysteresis effect prevents the catheter-tip to revisit its initial point when the tendon is released. This is the consequence of the plastic properties of the deflecting components when exposed to a large deflection.

C. Three-Dimensional Catheter-tip Trajectory

In traditional cardiac catheterization, catheter deflection can occur in only one plane if a single or double tendon system (two tendons for bidirectional types) is employed. In such a case, the catheter twist is unavoidable for reaching points along the catheter's longitudinal axis. Because of the flexibility of the catheter shaft and friction, twisting the catheter shaft at the insertion port depends on the energy stored in the flexible shaft and does not necessarily result in a predictable and repeatable rotation of the tip. The ability of the presented catheter to move the catheter tip in 3D is tested in the same experimental setup as for the 2D case but using all individual tendons and combinations of adjacent tendons. The experiment starts by actuating each of the four tendons individually in steps of 0.5 mm whilst recording the tip position with a magnetic tracking coil system. Then all possible combinations of driving adjacent tendons (in pairs of two) in parallel with variable step ratios covering the region between the two tendons; the resultant tip positions are recorded. In order to visualize the tip positions in 3D coordinates, the recorded cloud points are used to fit a mesh representing the reachable working space. Figure 15 shows

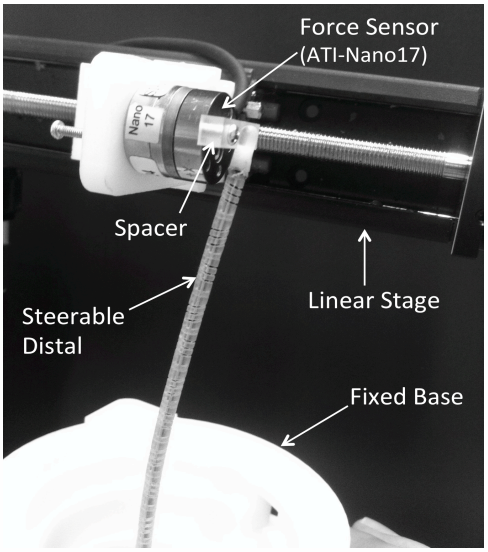

Fig. 16. Lateral force sensing experimental setup.

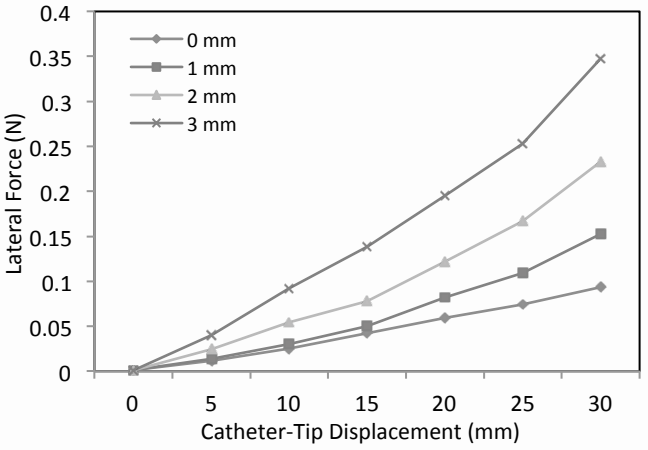

Fig. 17. Stiffness adjustability analysis using simultaneous tension in all four tendons. The top curve shows the catheter Force-Displacement diagram when the tendons are displaced 3 mm simultaneously compare to the three curves which are recorded when the tendon displacement is 2 mm, 1 mm, and without any applied tension (bottom curve).

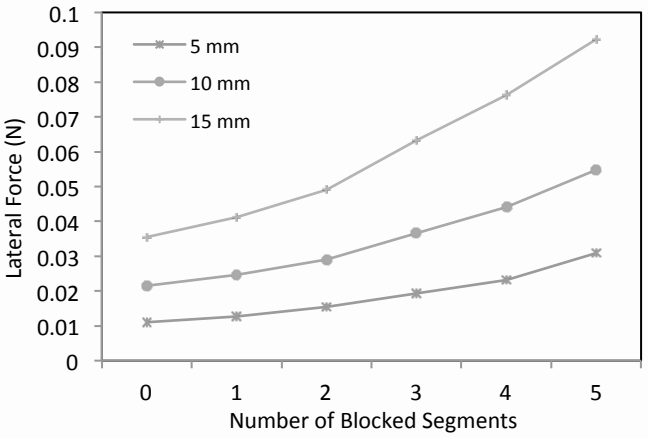

Fig. 18. Stiffness adjustability experimental results using length limiter axis and by modifying the length of the deflectable distal. The experiment is repeated for 3 different lateral displacements of the tip.

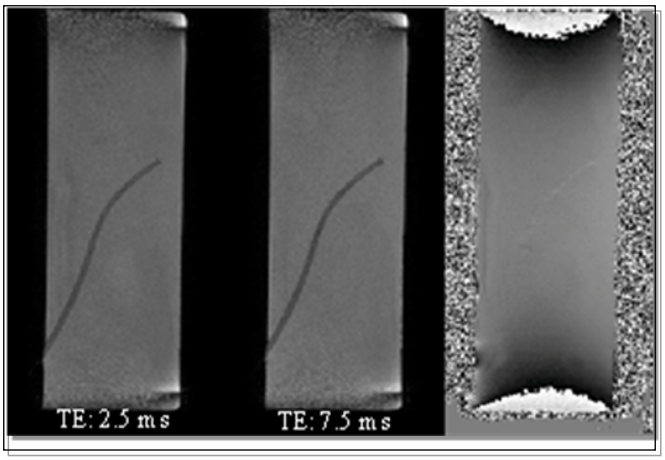

19. Two acquired images with different echo times (left) and calculated phase image (right).

the trajectory of the catheter-tip in 3D space. This experiment was carried out only for the catheter without any blocked segments (full deflectable length). Activating the length-limiter axis, more areas can be reached inside the workspace shown here.

D. Repeatability Result

The repeatability of the positioning is examined by choosing a point in the middle of the deflection range and manipulating the catheter to go to the same point from an initial position a number of times and recording the position values using the tracking system. In order to explore what happens if two tendons are operated at the same time, two adjacent tendons are displaced equally (5 mm) to reach a desired position in space. Then the position is recorded and the tendons are released allowing the catheter-tip to return to the initial state. The procedure is repeated 10 times and the tip positions in space are recorded. The maximum positioning repeatability error in X, Y, and Z axis are 0.494 mm, 0.759 mm, and 0.453 mm, respectively. The result shows the maximum standard deviation (square root of variance) from the desired point in 3D space is 0.762 mm. The tendon friction, tendon length variation due to stretching, and deformation of the assembly due to plasticity of the materials are assumed to be the source of the overall small error.

E. Stiffness Adjustability Result

In addition to the ability of reaching points in 3D space using its state-of-the-art three degrees-of-freedom design, the proposed catheter steering structure has the ability to adjust its stiffness. An equal increase in tension of the tendons increases the tension in the spiral segments and results in an increased stiffness in the steerable distal part. Despite the fact that the applied tension causes a small decrease in the length of the deflectable distal part, it increases the stiffness. The proper amount of contact force between the catheter-tip and the heart tissue is proved to play a key role in carrying out successful RF-ablation in the heart [21,22]. The proposed feature is proved by means of experiments studying the variations in lateral catheter stiffness. An experimental setup (see Fig. 16) is used to investigate the adjustability of the catheter stiffness; lateral forces are applied by moving the force sensor against the catheter-tip in steps of 5 mm. The experiment is repeated for different structural compression caused by simultaneous tendon displacements of 0 mm, 1 mm, 2 mm, and 3 mm. Fig. 17 shows four curves representing the tendon displacement under laterally applied forces for different compression conditions. The results show that by increasing the tension in all four tendons simultaneously the catheter stiffness increases significantly.

Another feature of the designed steering mechanism which can be employed for improving the stiffness and forcibility is the length limiter axis. In addition to modifying the workspace, the forcibility of the catheter increases when reducing the deflectable length of the catheter's distal end. A similar experiment is carried out to understand the effect of modified length on catheter forcibility. The lateral force applied by the catheter tip is recorded for six different length limiter axis configurations. The experiment is repeated for catheter-tip displacements of 5 mm, 10 mm, and 15 mm. Fig. 18 shows the experimental results and achieved increase in catheter forcibility.

F. MR-Compatibility Result

Since the prototype does not involve any electronic circuits or conductive materials, no interaction with the RF-coil of an MR-scanner is expected. The carbon fibers used in the steering mechanism have low conductivity (Tube: 400 Ω/m, Rod: 650 Ω/m) and also short length (Tube: 100 mm, Rod: 120 mm). Figure 19 shows the acquired images at two different echo times and the obtained phase difference image representing a map of the main field homogeneity in the phantom. The signal to noise ratio (SNR) of the acquired images of normal phantom and the catheter installed phantom are evaluated to be 51.3 in both images. The SNR was measured by considering the mean signal intensity within a small region-of-interest (ROI) and dividing by the standard deviation of noise calculated from background air [23] :

$$SNR_{signal} = 0.655 \times \frac{S}{\sigma_{air}}$$

The results confirm that the proposed catheter prototype does not affect the homogeneity of MR images.

VI. Discussion

In conventional catheters with a single DOF deflectable tip, the operator has to twist the catheter to access points around the catheter's longitudinal axis. Because of the use of long flexible shafts in catheters, twisting the shaft at insertion point does not necessarily have predictable results at the distal end. The energy stored in the flexible shaft makes it more difficult to move from one point in 3D space to another due to the unpredictable energy release in the shaft, which causes unexpected rotations at the catheter tip. This issue is addressed, in the present design where the twisting of the shaft is not required for catheter tip navigation. Thanks to its 2-DOF deflectable structure, the developed catheter presented here has the ability of deflection in all directions with regards to its longitudinal axis. This feature improves the tip positioning and

navigation by improving the maneuverability of the steerable mechanism. The hysteresis diagram indicates that in order to return the catheter back to the initial position after a large deflection the opposite tendon needs to be actuated. This is due to the large deflection. Therefore having two degrees of freedom provides the ability to deflect in opposite direction to overcome positioning error caused by hysteresis effect. At present, in order to modify the curvature or length of the deflectable part of the catheter, an external sheath is employed in commercial catheters. The additional sheath must be larger in diameter than the used catheter enveloping the catheter itself. However, in the presented catheter steering design a carbon fiber tube is used to modify the length of the deflectable part as a result of reducing the number of segments in action, yet the catheter outer diameter is not increased. This additional degree of freedom extends the workspace of the catheter and increases the forcibility.

In an EP ablation procedure, the adequate contact force between the catheter-tip and soft tissue is known to be an important factor for successful ablation [21,22]. In contrast to conventional catheters, the spiral structure of the catheter presented here is stiffness adjustable. Therefore, the operator can decide to increase the stiffness of the catheter where it is required by simply increasing the tension in all tendons simultaneously. MR-compatibility is achieved as a result of using MR-safe materials in the steering structure. The high positioning accuracy and the improved navigation efficiency are the most significant advantages of the proposed steering mechanism presented in this paper. Since in the present design the catheter lumen is filled with the carbon fiber rod and tube, the flexible sleeve which is located inside the central lumen of the catheter has to be replaced in future with a precisely extruded tubing to provide lumens for injection and other applications.

VII. Conclusions

A novel 3-DOF MR-compatible segment based steering mechanism for cardiac catheters has been created employing a high-resolution rapid prototyping technique. The proposed catheter steering mechanism can deflect in all directions away from its longitudinal axis thanks to its 2-DOF tendon driven segment structure. The deflectable length of the catheter can be adjusted using an insertable carbon fiber tube adding another degree of freedom to the steering mechanism yet not affecting the outer diameter of the device. Experimental results indicate that the catheter tip can be precisely navigated in 3D space employing four tendons without the need to twist the catheter shaft. In addition, the developed steerable mechanism is benefitting from being stiffness adjustable. The MR-compatible materials used in the steering mechanism of the catheter distal make it safe to be used for robot-based catheterization inside an MRI scanner. The proposed catheter steering mechanism represents the foundation to conduct entire cardiac catheterization procedures inside an MRI scanner using an autonomous MR-compatible robotic system controlled using MR imaging feedback. The MR-compatible robotic catheter actuation device is currently under development in our research group. This robot is based on hydraulic actuation in a master-slave hydraulic system. The preliminary result is promising but further improvement in positioning accuracy and actuation speed is necessary. For catheter-tip trajectory evaluation a magnetic tracking coil is used in this research, this is also planned to be replaced with an active MR tracking coil in future work where the catheter is to be used inside MRI scanner.

Acknowledgment

The authors thank Ms. Hanne Guthormsen and Mr. Jim Trotter for their invaluable assistance in designing the robotic actuator and conducting the experiments.

References

[1] J. Peirs, J. Clijnen, D. Reynaerts *et al.*, “A micro optical force sensor for force feedback during minimally invasive robotic surgery,” *Sensors and Actuators A: Physical,* vol. 115, no. 2-3, pp. 447-455, 2004.

[2] P. Polygerinos, A. Ataollahi, T. Schaeffter *et al.*, “MRI-Compatible Intensity-Modulated Force Sensor for Cardiac Catheterization Procedures,” *Biomedical Engineering, IEEE Transactions on,* vol. 58, no. 3, pp. 721-726, 2011.

[3] C. Yi*, et al.*, "Multi-turn, tension-stiffening catheter navigation system," in *Robotics and Automation (ICRA), 2010 IEEE International Conference on*, 2010, pp. 5570-5575.

[4] J. Driller, "Kinetics of magnetically guided catheters," *Magnetics, IEEE Transactions on,* vol. 6, pp. 467-471, 1970.

[5] P. Dupont, J. Lock, B. Itkowitz, and E. Butler, “Design and control of concentric-tube robots,” *Robotics, IEEE Transactions on*, vol. 26, pp. 209 –225, april 2010.

[6] M. A. Martinelly and W.C. Haase, ”Method and system for navigating a catheter probe,” U.S. RE40,852, July 14, 2009.

[7] Sheldon D. Gould and Garry T. Riggs, “Curving Tip Catheter,” U.S. Patent 4,586,923, May 6, 1986.

[8] M. Eng, R. R.Viswanathan, P. R. Werp, I. Tunay, A. K. Pandey, and G. T. Munger, “Electrophysiology Catheter,” U.S. Patent 6,980,843, Dec. 27, 2005.

[9] P. Kanagaratnam*, et al.*, "Experience of robotic catheter ablation in humans using a novel remotely steerable catheter sheath," *Journal of Interventional Cardiac Electrophysiology,* vol. 21, pp. 19-26, 2008.

[10] R. Razavi*, et al.*, "Cardiac catheterisation guided by MRI in children and adults with congenital heart disease," *The Lancet,* vol. 362, pp. 1877-1882, 2003.

[11] T. Schaeffter and H. Dahnke, "Magnetic Resonance Imaging and Spectroscopy," in *Molecular Imaging I.* vol. 185/1, W. Semmler and M. Schwaiger, Eds., ed: Springer Berlin Heidelberg, 2008, pp. 75-90.

[12] J. E. Mackewn*, et al.*, "Performance Evaluation of an MRI-Compatible Pre-Clinical PET System Using Long Optical Fibers," *Nuclear Science, IEEE Transactions on,* vol. 57, pp. 1052-1062, 2010.

[13] RJ. Lederman, “Cardiovascular interventional magnetic resonance imaging,” in *Circulation,* 2005, PP-3009-17.

[14] A. Tzifa, T. Schaeffter, R. Razavi, “MR imaging-guided cardiovascular interventions in young children*,” in Magn Reson Imaging Clin N Am*, 2012, PP-117-28.

[15] SR. Dukkipati, *et al.,* “Electroanatomic mapping of the left ventricle in a porcine model of chronic myocardial infarction with magnetic resonance-based catheter tracking,” *in Circulation,* 2008, vol.118, PP-853–862.

[16] M. Bock, FK. Wacker, “MR-guided intravascular interventions: techniques and applications,” *in J Magn Reson Imaging*, 2008, PP-326-38.

[17] MK. Konings, LW. Bartels, HFM. Smits, CJG. Bakker, “Heating around intravascular guidewires by resonating RF waves,” in J Magn Reson Imaging, 2000, PP-79–85.

[18] S. Weiss, *et al*. “In vivo evaluation and proof of radiofrequency safety of a novel diagnostic MR-electrophysiology catheter,” *in Magnetic Resonance in Medicine*, 2011, PP-770–777.

[19] "Artisan Extend™ Commercial Catheter Developed by Hansen Medical" Internet: http://www.hansenmedical.com/us/products/ep/artisan-control-catheter.php
[20] "AURORA EM Tracking System Specification Brochure." Internet : http://www.ndigital.com/medical/documents/aurora/aurora-brochure.pdf
[21] VY. Reddy, *et al.*, " The relationship between contact force and clinical outcome during radiofrequency catheter ablation of atrial fibrillation in the TOCCATA study," in Heart Rhthm, Nov.9(11), 2012, PP-1789-1795.
[22] A. Thiagalingam, et al., " Importance of Catheter Contact Force During Irrigated Radiofrequency Ablation: Evaluation in a Porcine *Ex Vivo* Model Using a Force-Sensing Catheter," in Journal of Cardiovascular Electrophysiology, 2010, Vol. 21, PP-806-811.
[23] L. Kaufman, et al., " Measuring signal-to- noise ratios in MR imaging," in Radiology, 173, 1989, PP-265-267.

Asghar Ataollahi received the B.Sc. degree in electrical engineering and control systems from K. N. Toosi University of Technology, Tehran, Iran, and the M.Sc. in mechanical engineering research from the King's College London, London, U.K., where he is currently working toward the Ph.D. degree. He specializes in medical robotics as a member of Centre for Robotics Research (CORE) and collaborates with cardiologists and urologists at St.Thomas' Hospital and Guy's Hospital, London.

Rashed Karim received his B.Sc degree in Computer sciences from the University of Toronto in 2002 and his M.Sc degree in advanced computing in 2005. From 2005 to 2009, he was with the Department of Computing, Imperial College London, where he was involved in developing image processing algorithms with applications in cardiac MRI images. He was awarded a Doctor of Philosophy degree in left atrium segmentation from cardiac MR images. Since 2010, he has been working as a Postdoctoral Research Fellow investigating several problems in cardiac image processing. In particular, problems arising in image segmentation, 3D visualization and image guidance.

Arash S. Fallah is a Research Associate in structural engineering at Imperial College London specialising in computational and analytical modelling of blast and impact loaded monolithic, composite and hybrid structures and systems. His interests include frequency filtering in phononic metamaterials and lattices, extended finite element formulation of plated structures, nonlinear dynamics and chaos, damage and fracture in composites and constitutive visco-elastic, plastic and visco-plastic formulations for metals and composites. Much of his work is funded by EPSRC, Dstl/MoD, Health and Safety Executive and the Office of Naval Research Global and is conducted in collaboration with University of Cape Town and US Naval Academy.

Kawal Rhode received the B.S. degree in basic medical sciences and radiological sciences from King's College London, London, U.K. in 1992. From 1998 to 2001, he was with the Department of Surgery, University College London, where he was engaged in investigating quantitative blood flow analysis using X-ray angiography as part of his Doctor of Philosophy degree. From 2001 to 2007, he was a Postdoctoral Research Fellow in the Division of Imaging Sciences, King's College London, where he was involved in image-guided interventions, particularly catheter-based electrophysiology procedures, and has been an Assistant Professor in the Division since 2007. He has authored or coauthored more than 100 publications in journals, conference proceedings, and book chapters, and holds several patents. His research interests include image-guided cardiovascular interventions, cardiac eletrcomechanical modelling and computer simulation of minimally invasive procedures.

Lakmal D. Seneviratne (M'05) received the B.Sc.(Eng.) and Ph.D. degrees in mechanical engineering from the King's College London, London, U.K. He is currently a Professor of robotics at Khalifa University, Abu Dhabi, UAE, on secondment from King's College London, where he is a Professor of mechatronics. His current research interests include robotics and autonomous systems. He has authored or coauthored more than 250 refereed research papers related to robotics and mechatronics.
Prof. Seneviratne is a Fellow of both the Institution of Engineering and Technology (IET) and the IMechE.

Reza Razavi received the M.D. degree on MR Guided Cardiac catheterization from the King's College London, London, U.K. He studied medicine at St. Bartholomew's Hospital Medical School, University of London, London. He trained in Paediatrics and Paediatric Cardiology at Guy's and St. Thomas' Hospital London. He was a Clinical Research Fellow. He was appointed as a Lecturer and a Honorary Consultant in Paediatric Cardiology in August 2001, and a Professor of Paediatric Cardiovascular Science in October 2004. He has been the Deputy Head of the Division of Imaging Sciences since January 2005 and the Head of Division since January 2007. He is the Director of the KCL Centre for Excellence in Medical Engineering funded by the Welcome Trust and Engineering and Physical Sciences Research Council. His current research interests include cardiovascular MRI- and MR-guided cardiac catheterization.

Tobias Schaeffter studied electrical engineering in Berlin and received the Ph.D. degree in magnetic resonance imaging (MRI) from the University of Bremen (Prof. Leibfritz), Bremen, Germany. From 1996 to 2006, he was a Principal Scientists at the Philips Research Laboratories, Hamburg, Germany. In April 2006, he took up the post as the Philip Harris Professor of imaging sciences at the King's College London, London, U.K. His current research interests include the investigation of new acquisition and reconstruction techniques for cardiovascular and quantitative MRI. In particular he works on new techniques for MR-guided electrophysiology procedures, and the quantitative assessment of ablation procedures.interests in minimally invasive surgery and robotics. He has also pioneered a technique for Botulinum toxin injection for the treatment of overactive bladders.

Kaspar Althoefer (M'03) received the Dipl.-Ing. Degree in electronic engineering from the University of Aachen, Aachen, Germany, and the Ph.D. degree in electronic engineering from King's College London, London, U. K. He is currently a Professor with the Department of Informatics, King's College London. He has extensive expertise in robot-based applications, sensing, and embedded intelligence. He has authored or coauthored more than 150 refereed research papers related to mechatronics and robotics.